Organic phosphorus compounds as heat release regulators in hardening shielding concrete

Roman Jaskulski [a],[*], Michał A. Glinicki [b], Zbigniew Ranachowski [b], Wojciech Kubissa [a]

[a] Faculty of Civil Engineering, Mechanics and Petrochemistry, Warsaw University of Technology, Łukasiewicza 17, 09-400 Płock, Poland
[b] Institute of Fundamental Technological Research, Polish Academy of Sciences, Pawińskiego 5B, 02-106 Warsaw, Poland

HIGHLIGHTS

- Phosphorous compounds lower the temperature gradient in hardening shielding concrete.
- The lower thermal conductivity of aggregate the higher temperature gradient decrease.
- Maximum temperature of hardening shielding concrete stays not affected.

ARTICLE INFO

ABSTRACT

The paper presents the results of the study of the influence of the addition of retarding superplasticising admixture based on triisobutyl phosphate and modified phosphonates on the amount of heat generated by hardening shielding concrete. A four-point measurement of the heat generated during the hardening of concrete with an admixture dose of 0, 0.5, 1.0 and 2.0% by weight of the cement was made and the concurrent measurement of the heat released by the hardening cement paste was measured with an isothermal calorimeter. Based on the results from the calorimeter, the effect of the admixture on the temperature field in the hardening concrete mass elements was simulated for different aggregates.

The results indicate that the admixture clearly lowers the temperature gradient in hardening mass concrete. In the simulations, the most clear effect was achieved in the case of concrete with barite aggregate, where the gradient value was reduced from 10°C/m to 8°C/m for an admixture content equal to 2.0%.

© 2019 Elsevier Ltd. All rights reserved.

1. Introduction

Organic phosphorus compounds (i.e. phosphates and phosphonates) are known and used in concrete technology as water reducers and set retarders [1–5]. Their action consists of modifying the course of the cement hydration process, which allows the start of concrete setting processes to be delayed. They can also slow down and prolong the process of the setting and hardening of the concrete, which helps maintain the assumed workability of the concrete mixture for the time needed to transport, stack and compact the concrete mix. Using these compounds, which prolongs cement hydration, results in the amount of heat released in this process per unit of time being reduced.

The control of the amount of heat released during the setting and hardening of concrete is an important issue in the case of massive structures. Due to the large cross-sections of elements and the relatively low thermal conductivity of concrete, a significant amount of heat resulting from the hydration of cement accumulates in the concrete mass, and at the same time raising its temperature [6–8]. In [9], the authors draw attention to the particular importance of controlling heat production during the construction of shielding structures. Because the thickness of shielding concrete is usually from 1 to 3 m, the heat release during the hydration of cement results in the generation of a temperature gradient inside the concrete. The gradient induces thermal and autogenous strains which are associated with the differential degree of cement hydration. The magnitude of the resulting stresses depends on the current stiffness of the hardening concrete. As long as the concrete does not start to set, stresses do not arise, and when setting begins, the magnitude of stress increases with the increasing stiffness of the concrete. If, at some point, the temperature gradient generates a stress greater than the current concrete tensile strength, cracks appear. Paper [10] is focused on the behaviour of early-age concrete in massive structures in relation to the prediction of both cracking risk and residual stresses. A 3D thermo-chemo-

mechanical model implemented in a Finite Element code has been developed on the basis of complete material characterization experiments.

In extreme cases, if an efficient removal of heat from a massive element is not ensured, the temperature in its interior reaches 70–75°C [6,7,11]. Such a high temperature adversely affects the quality of the concrete and is the cause of delayed ettringite formation (DEF) [6,7,11]. It also causes thermal cracks that reduce the strength and tightness of the concrete. The latter is a result of the occurrence of temperature gradients in massive concrete elements, which in turn cause tensile stresses. Moreover, such temperature gradients can also cause damage in young concrete if it has not yet achieved a sufficiently high tensile strength.

The effects of the excessive heating of a massive concrete element, or uneven temperature distribution in its interior are particularly undesirable in the case of shielding concrete used to provide biological shields in nuclear power plants. Because of their dimensions, the biological shields are always massive structures. Their task is to reduce the ionizing radiation intensity resulting from nuclear fuel fission processes to safe levels. Another role is to separate the reactor from the environment and prevent, in the event of a breakdown, the leakage of harmful gases, radioactive vapour or other hazardous substances. In order to effectively fulfil this role, the concrete in shielding construction must be highly impermeable to gases and liquids. This condition can only be met by a material in which thermal cracks have not occurred.

To avoid the effects of excessive growth and uneven temperature distribution in a massive concrete element, cements with a low heat of hydration, as well as various technological and technical treatments, are used. These include the cooling of concrete components (mainly aggregates) in order to obtain a mixture of a low initial temperature, the placing of cooling installations in a concrete mass, as well as the isolation of exposed fragments of a concrete structure in order to minimize temperature gradients. These treatments, combined with the computer simulation of their effects, can be the basis for controlling the temperature fields arising in concrete during its hardening. Such attempts have already been made [12].

A commonly used method of limiting temperature gradients in massive concrete structures is the use of binders with mineral additives (e.g. fly ash), which are characterized by a lower hydration heat than Portland cement without additions. Research on the properties of such binders, including the amount and rate of heat released by them during hydration, together with the more and more accurate 3D numerical simulations of the structure, allow for the effective reduction of temperature gradients and the minimization of the possibility of cracks and other adverse phenomena occurring during concrete hardening [13–17].

It is also possible to change the intensity of heat release during hydration by using natural zeolites [19]. The effect varies depending on the type of cement and the amount of zeolite used. Changes in heat release during hydration can also be caused by the application of the used ceramic sorbents that have lead absorbed on them [20].

Another solution may lie in influencing the cement hydration process by using appropriate admixtures to extend the setting time and thereby reduce the amount of heat released in a unit of time. Substances suitable for this application appear to be organic phosphorus compounds, which both delay and extend the hydration process of cement [1,5]. Delaying hydration can range from a few to even tens of hours. Its elongation may be significant enough to substantially reduce the power released by the hydrating cement, which may have a visible effect on the value of the maximum gradient arising in the massive concrete structure.

The use of concrete admixtures to reduce temperature gradients in massive concrete constructions is a relatively new issue.

The use of this method in practice requires research primarily aimed at determining the achievable effects using the doses of admixtures recommended by the manufacturers, which do not lower the mechanical parameters of the concrete, and in particular its strength. It is also worth investigating the use of dosages larger than those recommended while balancing the possible beneficial effects and their negative impact on the properties of hardened concrete, including its microstructure [2,18].

This paper presents the results of research on the influence of admixtures based on modified phosphonates on the thermal parameters of the setting and hardening process of shielding concrete. Particular emphasis was placed on temperature gradients arising in massive reinforced concrete elements. The tests were carried out on the same concrete mixtures using two methods. The first of these is the method of measuring the changes in the temperature of hardening concrete described in [21]. Based on the results obtained using this method, as well as others, the values of the maximum temperature gradient arising in the hardening concrete mixture were calculated. In the second method, an isothermal calorimeter I-Cal 2000 HPC was used to obtain the values of the function of the heat energy released by the setting and hardening cement paste. The values obtained in this way were then used to simulate the temperature field in the hardening massive concrete block. Computations in the Comsol program were made for this purpose. Simulations were carried out by adopting four types of shielding concrete: one using amphibolite aggregate (reference mixture), and three using aggregates used in shielding concrete technology. Based on the simulation results, the maximum temperature gradient values were calculated, as in the case of temperature measurements in concrete using the first method. These values were then analysed in terms of their dependence on the amount of admixture used and the type of aggregate in the concrete.

2. Materials and methods

2.1. Mix compositions

The concrete used in the tests was made using serpentinite aggregate, which is used in shielding concrete technology due to the high content of chemically bound water. Four concrete mixtures were prepared, differing in terms of their retarding admixture content. The admixture was a commercially available mixture based on modified phosphonate (APP) which contained 70% of water and 30% of dispersed solids. Triisobutyl phosphate (about 1 wt%) was another component of the mixture.

Specimens of the paste tested in an isothermal calorimeter have the same w/c ratio as concrete mixtures and the same amount of retarding admixture related to the weight of the cement. In the case of both the concrete and the paste, the special cement CEM I 42.5 R SR-5/LH/NA was used. The chemical composition of the cement is presented in Table 1 and more properties are described in detail in [22].

As fine aggregate, quartz sand of the 0–2 mm fraction in the amount of 20% of the volume of the aggregate composition was used. The remaining part was coarse aggregate composed of two fractions of crushed serpentinite: 2–8 mm and 8–16 mm. Ordinary tap water was used which meets the requirements of the PN-EN 1008:2004. The compositions of the concrete mixtures are shown in Table 2.

Table 1
Chemical composition of the cement [22].

Component	Content [mass %]
L.O.I.	1.12
SiO_2	21.48
Al_2O_3	4.80
Fe_2O_3	2.62
CaO	65.60
MgO	0.87
SO_3	2.84
K_2O	0.47
Na_2O	0.12
Cl	0.008

Table 2
The composition of concrete mixtures.

| Component	C0	C05	C10	C20
Cement [kg/m^3]	416	416	416	416
Water [kg/m^3]	208	206	204	200
Quartz sand 0–2 mm [kg/m^3]	574	574	574	574
Serpentinite aggregate 2–8 mm [kg/m^3]	880	880	880	880
Serpentinite aggregate 8–16 mm [kg/m^3]	317	317	317	317
Retarding admixture [% of cement mass]	0	0.5	1.0	2.0

The mixtures were prepared in a counter-rotating mixer. The volume of each batch was about 0.01 m^3. First, the dry ingredients were mixed together, and then water with admixture was added. The time of contact between the water and cement was recorded. After the addition of the water, the mixture was mixed for about 5 min and then placed in a special insulated form (tube) equipped with temperature sensors. The mixture was laid in two layers and each layer was densified on a vibrating table.

2.2. Experimental methods

Determination of the temperature changes in the hardening cement mixture was performed with the use of specially developed equipment described in detail in [23]. It consisted of a cylindrical PVC chamber, with an inner diameter of 96 mm and a height of 500 mm (Fig. 1), insulated with two layers of 10 mm polyethylene foam. The top of the chamber was left open and was only covered with thin polyethylene foil to prevent the concrete mixture from losing moisture.

The temperature in the chamber was measured in four points with the use of sensors placed along the symmetry axis of the cylinder 50 mm, 200 mm, 350 mm and 500 mm above the bottom of the chamber. A self-designed electronic controller and interface were used to record the measurements. After the test was completed, the data was sent to a PC set. On the basis of the data, the temperature values were calculated in intervals of 60 s with an accuracy of 0.1 °C. The test lasted for up to 120 h after the casting of the concrete. The exemplary graph of temperature changes for the C0 concrete mixture is presented in Fig. 2.

The data recorded during 120 h of concrete hardening was then analysed in order to calculate the maximum value of the temperature gradient formed in the young concrete. Other parameters were also determined, such as: maximum temperature increase, maximum rate of the temperature increase and the time it was
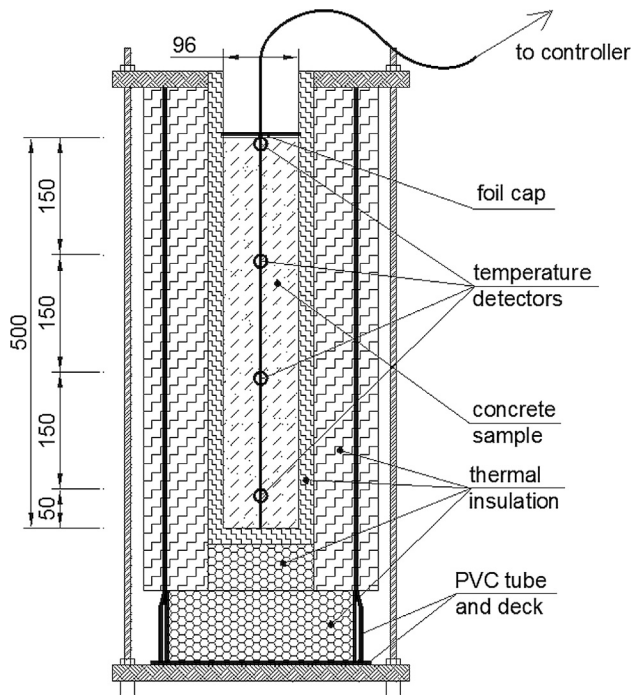
Fig. 1. The scheme of the testing equipment [23].
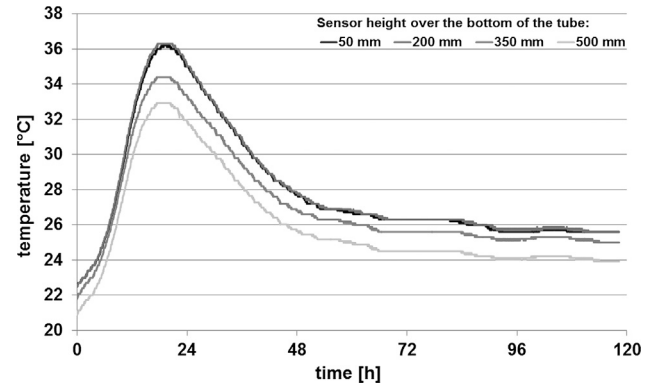
Fig. 2. Results of temperature measurements of the C0 hardening concrete mixture.

reached, and the time of reaching half of the maximum temperature increase (both in the case of the growth and decrease of its value). The above parameters were used for further analyses.

The calorimetric tests were carried out on specimens of cement paste with a mass of approx. 120 g, including 80 g of cement and 40 g of water, which meant the value of w/c = 0.5, as in the case of the concrete mixtures described earlier. The cement was mixed with water, in which the appropriate amount of admixture had previously been dissolved: 1, 2 or 4%. The paste specimens were placed in an isothermal calorimeter within a few minutes after contact of the cement and water. The equipment was turned on 24 h before the test in order to stabilize the temperature at the assumed level of 25 °C. The test lasted for 120 h, and the measured parameters were recorded every 60 s. The curves showing the heat released by the hardening cement paste obtained as a result of the measurements were then used in the temperature simulations of concrete blocks.

Computer simulations of temperature fields were performed to determine the relationship between the thermal properties of the concrete (resulting from the use of aggregates with different thermal properties), as well as the amount of added admixture and the obtained maximum values of the temperature and temperature gradient in a massive concrete block. The simulations were carried out using the Comsol program. As a model, a concrete block measuring 1000 × 1000 × 1000 mm was used that, with the exception of the upper surface, was insulated with a 100 mm layer of polystyrene. The assumed coefficient of heat transfer from the top surface of the concrete block was equal to 7 W/m^2·K, and from the surface of insulated surfaces was equal to 5 W/m^2·K. The thermal parameters of the concrete mixtures used in the simulations (i.e. specific heat and thermal conductivity coefficient) were determined using the transient method with the use of ISOMET 2114 equipment [24] on specimens of hardened concrete that were fully saturated with water. In order to simplify the simulation, it was assumed that these parameters remain constant during the concrete hardening. The measured values of these parameters, which were then adopted in the simulations, are summarized in Table 3.

In order to calculate the temperature gradient values, four points were defined in the simulated concrete block, the temperature of which was recorded after each calculation step. The location of the points is shown schematically in Fig. 3. In the simulations, a calculation time step of 900 s was adopted, and the calculations were carried out until the age of the simulated block reached 96 h.

3. Results and discussion

3.1. Experimental measurements

The results of the temperature measurements of the concrete mixtures, using the device presented in Fig. 1, were analysed. The results of the analysis are presented in Tables 4 and 5, and also

Table 3
Thermal properties of concrete mixtures used in the simulations.

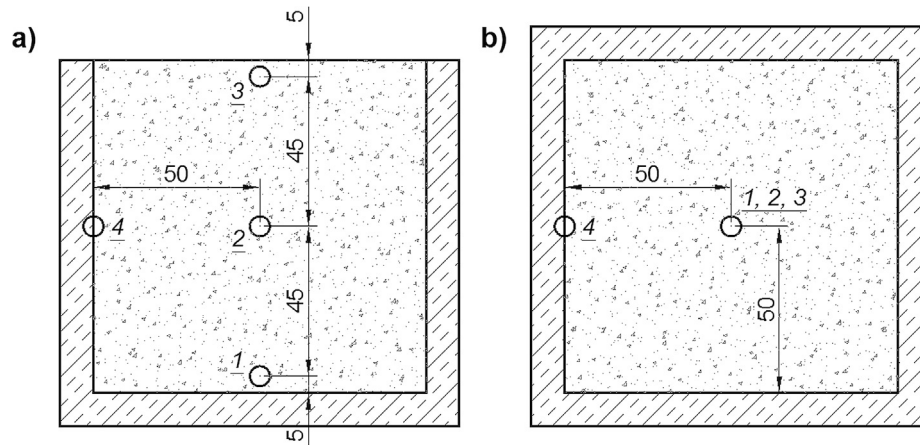| Concrete mixture with:	Bulk density ρ [kg/m^3]	Thermal conductivity λ [W/(m·K)]	Specific heat C_p [J/(kg·K)]
amphibolite aggregate	2530	2.23	765
barite aggregate	3210	1.87	590
magnetite aggregate	3550	3.13	590
serpentinite aggregate	2365	2.30	810

Fig. 3. Location of temperature measurement points (marked as 1, 2, 3 and 4) in the simulated blocks: a) side view, b) top view.

in Figs. 4–6. Due to the different initial temperature of each mix, instead of the absolute temperature values, the temperature rise in relation to its initial value was analysed. The value of the maximum temperature increase was determined while analysing the results of the measurements in three out of four points (results from the height of 500 mm above the bottom of the tube were omitted). The time of the maximum temperature increase was also determined.

In addition to the above-mentioned two characteristics, the time of the mixes achieving half of the maximum temperature rise was also determined. By subtracting this time from the time of the maximum temperature increase, the value was calculated that allows the rate of energy release by the hydrating cement in individual mixtures over a longer period to be compared. The results of the calculation of all the above-mentioned parameters are shown in Table 4, and the maximum values of the temperature increase are presented in Fig. 4.

The values of the maximum temperature increase indicate a negligible effect of the admixture dose on this value. It is possible to notice a certain trend, which is characterized by the maximum
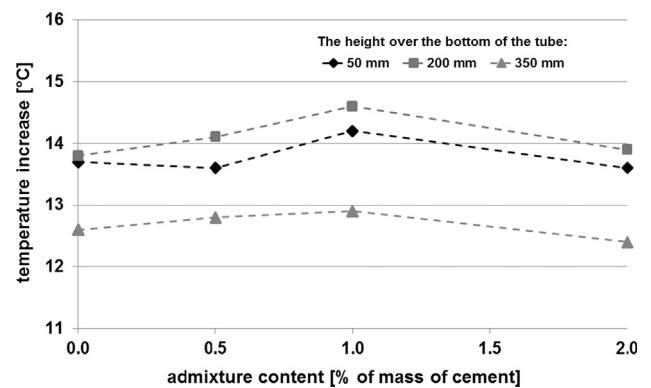

Fig. 4. The maximum values of the temperature increase obtained from the experimental measurements.

achieved value when adding 1.0% of admixture. However, due to small differences between the temperature rise values it is difficult to conclude that this is not an accidental pattern of the values.

Table 4
Parameters of the temperature increase of the mixtures.

Parameter	Measurement height	Mixture designation			
		C0	C05	C10	C20
Value of the max. ΔT [°C]	50 mm	13.7	13.6	14.2	13.6
	200 mm	13.8	14.1	14.6	13.9
	350 mm	12.6	12.8	12.9	12.4
Time of the max. ΔT [h]	50 mm	19.3	26.3	34.0	43.3
	200 mm	19.2	26.2	34.0	42.9
	350 mm	18.9	26.2	33.9	42.6
Time of 50% of the max. ΔT [h]	50 mm	11.5	15.6	23.5	31.1
	200 mm	9.8	15.7	23.7	31.2
	350 mm	9.4	15.9	23.8	30.5
Time interval between the max. ΔT and 50% of the max. ΔT [h]	50 mm	7.8	10.7	10.5	12.2
	200 mm	9.4	10.5	10.3	11.7
	350 mm	9.5	10.3	10.1	12.1

Table 5
The maximum instantaneous temperature rise and the time of its occurrence (experimental).

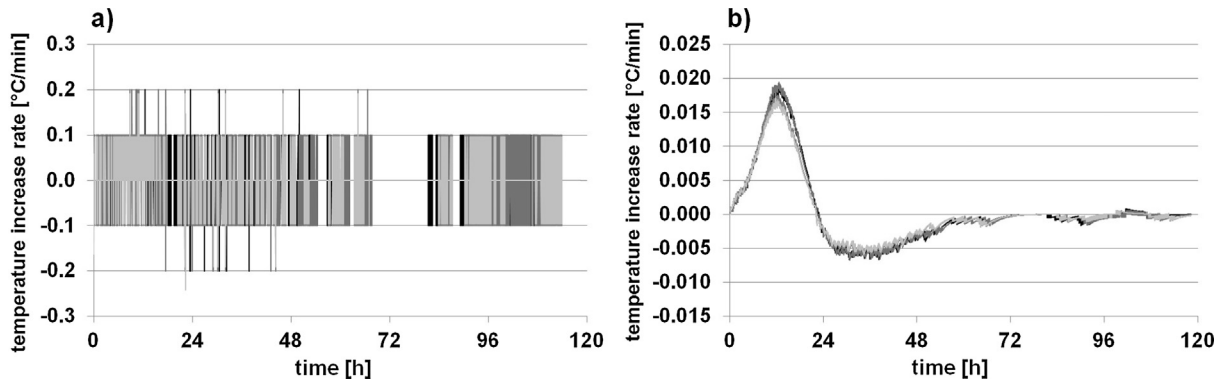| Parameter	Measurement height	Mixture designation			
		C0	C05	C10	C20
Max. value of ΔT/t [°C/h]	50 mm	1.13	0.88	0.86	0.73
	200 mm	1.17	0.93	0.91	0.76
	350 mm	1.08	0.86	0.83	0.68
The time of max. ΔT/t [h]	50 mm	12.7	18.2	27.6	38.2
	200 mm	12.7	19.7	28.4	37.5
	350 mm	11.8	19.5	28.2	36.2

Fig. 5. Temperature increase in the SP0 mixture: a) rough, b) after Brown's simple exponential smoothing.
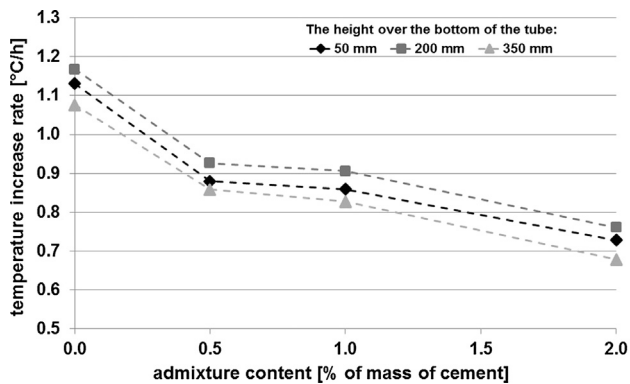

Fig. 6. The maximum rate of the temperature rise.

Similar temperature increases (about a dozen degrees Celsius) were found in the measurements and simulations carried out during the hardening of the foundation slab with a thickness of 35 cm [25,26]. There results were obtained as a solution of a one-dimensional (1D) non-linear heat transfer problem along the thickness of the slab.

In the case of the time of reaching the maximum temperature increase and the time of reaching half of the increase, the impact of the mixture on both values is very clear. Both times increase with an increasing amount of admixture. However, the interval between them first increases markedly after the addition of 0.5% of admixture, then it does not change after doubling the dose, and then again it increases significantly after increasing the dose to 2.0% of the cement mass.

The rate of temperature increase during the hardening of the mixtures was also analysed. Table 5 shows the values of the maximum instantaneous temperature increase and the time of its occurrence. They are selected from the smoothed values of differences in the results of the measurements of temperature made at 1 min intervals. In order to limit the impact of accidental changes and to better visualize the trend, the raw values of temperature increases were subjected to the Brown's simple exponential smoothing procedure. The value of the smoothing parameter $\alpha = 0.0045$ was determined iteratively by calculating the smallest squared error of expired forecasts. Fig. 5 presents the graphs of the raw values of the temperature increments and values obtained from the exponential smoothing procedure in the case of the C0 mixture.

Table 5 is limited to the values obtained on the basis of temperature measurements made at heights of 50, 200 and 350 mm over the bottom of the test tube. The results measured at 500 mm from the bottom were omitted because they showed high instability and variability, which resulted from the direct and significant influence of the ambient temperature changes.

The results given in Table 5 indicate the significant effect of the dose of the admixture on the maximum rate of the temperature rise. This influence is very similar for all the analysed measurement points. After the addition of 0.5% of admixture, the maximum rate of temperature increase drops by about 0.24°C/h, while doubling the dose causes a further decrease, which this time was insignificant (around 0.02°C/h). Finally, the next doubling of the dose (up to 2%) again causes a clear decrease of about 0.14°C/h. To sum up, compared to the mixture without the admixture, adding it in the amount of 2.0% of the cement mass causes the drop in the maximum rate of temperature increase by an average of 0.41°C/h, i.e. about 35% in comparison to the concrete mixture without the admixture.

The effect of the admixture dose at the time of achieving the maximum rate of temperature rise is also clear. The relationship is almost linear, which can be clearly seen in Fig. 6. Due to the probable existence of a physical limitation of the maximum delay, it should be assumed that it seeks some limit value, which may be indicated by the decreasing slope of the last section of the plotted polygonal chain.

On the basis of the temperature values measured at three points, the temperature gradient values were also calculated. The calculation did not take into account the temperature measured at 500 mm above the bottom of the test tube. The maximum gradient in all cases appeared between measuring points located at heights of 200 and 350 mm. A graph of the changes in the value of the gradient is shown in Fig. 7.

The obtained results of the temperature gradient calculations indicate that the amount of applied admixture influences this parameter. They also suggest that this effect is not proportional to the amount of used admixture, and at higher doses the gradient no longer drops.
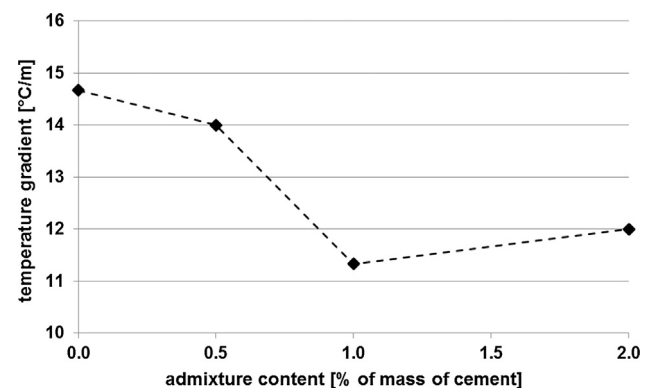

Fig. 7. Values of the maximum gradient of temperature obtained from experimental measurements.

3.2. Isothermal calorimetry

The results of the isothermal calorimetry are presented in Fig. 8. Four cement paste mixtures with different admixture doses were examined and the difference in the heat release course is clearly visible. It can be seen that the higher the dose is, the later the maximum value of heat release rate occurs. What is more, the maximum value decreases with an increasing dose of the admixture, although between 1.0% and 2.0% the difference is negligible.

The obtained curves of heat flow were also analysed in the way presented in [27] and [28] where some characteristic points of the curve are picked up (see Fig. 9): A – the end of induction period, B – the maximum instantaneous heat release rate, and C – the maximum value of heat release. On the basis of the values, some characteristic parameters are calculated, which are shown in Table 6 for the curves presented in Fig. 8.

In comparison to the results presented in [28], where the inter alia retardation effect of modified PCE-based superplasticisers was investigated, the tested admixture shows much stronger retarda-
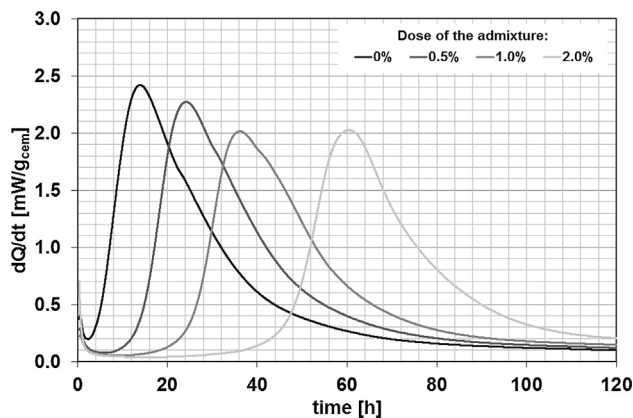
tion. The t_A time (end of induction period) is several times higher. For the maximum dose of the admixture of 2.0% (0.6% of solid), the end of induction period t_A occurred after 16 h compared to ab. 2.5 h in the case of the cement paste without the admixture. For PCE-based superplasticizers used in a dose of 0.5% of solid polymer, the highest obtained retardation of t_A was 5 h. It was mentioned above that the tested phosphonate-based admixture decreases the maximum heat generation rate, while the tested PCE-based superplasticisers clearly increase this characteristic value.
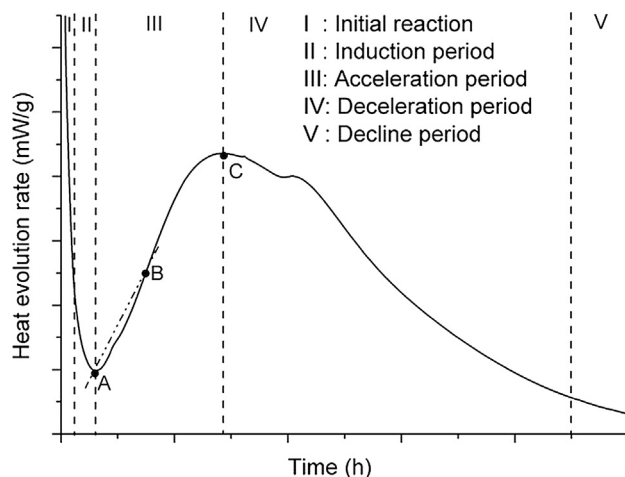
In [27], different modified PCE-based admixtures were investigated and the influence of some of them on cement hydration was also tested. As far as the end of the induction period is concerned, the results are close to those presented in [28] and they significantly differ from the values presented in this paper. However, if the maximum instantaneous heat increase rate is compared, the changes can be seen to be similar to those obtained with the use of the phosphonate-based admixture. The polymer denoted as PSSS decreased the heat peak value by 7% (comparable to 6% in the case of the 0.5% dose of the admixture), and the one denoted as PAA by 14% (comparable to 16 and 17% in cases of the1% and 2% dose of the admixture respectively). Unfortunately, there is no information in the paper concerning the dosing of the used superplasticisers in isometric calorimetry tests. It is only mentioned that the doses in all the tests were 0.1, 0.2 and 0.4% of the solid polymers by the weight of cement. Therefore, a direct comparison is difficult.

In [29], the use of superplasticizers: sulfonated melamine–formaldehyde condensate (SMF), sulfonated naphthalene-formaldehyde condensate (SNF), polycarboxylate (PC) and polycarboxylate ether (PCE) is presented. A reduction of the hydration heat of fly ash blended cement and prolongation of the initial setting time by 5% to 16% was obtained. The initial setting time of the control cement CEM II/A-V 42.5R is 252 min, whereas that of the cement with the addition of PCE and PC is respectively 266 and 275 min (prolongation respectively by 5% and 9%), and the cement with the addition of SMF and SNF is respectively 292 and 286 min (prolongation respectively by 16% and 13%). It can also be seen in Fig. 10 that the retardation effect is almost nothing in comparison to the phosphonate-based admixture.

The influence of chemical admixtures on the heat release during hydration of concrete made of CEM I 42.5 R with the addition of
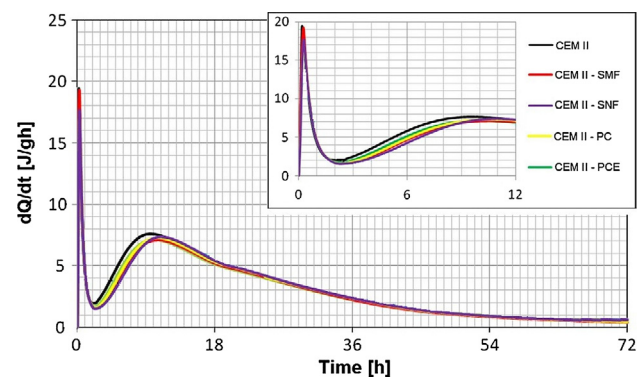

Fig. 8. Calorimetric curves of the cement paste with different mixture doses.

Fig. 9. A typical exothermic heat flow curve of cement hydration [27].

Fig. 10. Calorimetric curves of fly ash blended cement pastes tested in [29].

Table 6
Parameters of cement hydration extracted from the calorimetry curves.

Dose of the admixture	t_A [h]	$(dQ/dt)_A$ [mW/g]	Q_A [J/g]	$(dQ/dt)_B$ [mW/g]	K_{A-B} [mW/gh]	$(dQ/dt)_C$ [mW/g]	Q_{A-C} [J/g]
0.0%	2.42	0.195	1.85	1.244	0.192	2.421	54.27
0.5%	6.25	0.076	2.51	1.345	0.105	2.273	57.31
1.0%	11.02	0.054	3.03	1.304	0.064	2.016	56.20
2.0%	16.42	0.037	4.91	1.322	0.029	2.025	72.56

rice husk ash (RHA) and limestone filler was presented in [30]. The three types of chemical admixtures used in this research were obtained from commercial manufacturers – one PCE, and two LS products – a liquid-based superplasticizer showing retarding effects (LS-ret) and a powder-based admixture showing accelerating effects (LS-acc). A delay was observed in the initial setting time and a reduction in the amount of heat released in the initial period was seen in the case of the LS-acc and LS-ret admixtures. In particular, LS-ret caused a delay of the initial setting time of up to 72 h. It was also observed that the higher the RHA replacement, the smaller the retardation effect. From this conclusion, one may assume that if blended Portland cement is used, the admixture effect on the temperature gradient in mass concrete structures can be weakened, which opens the way for further research in the area.
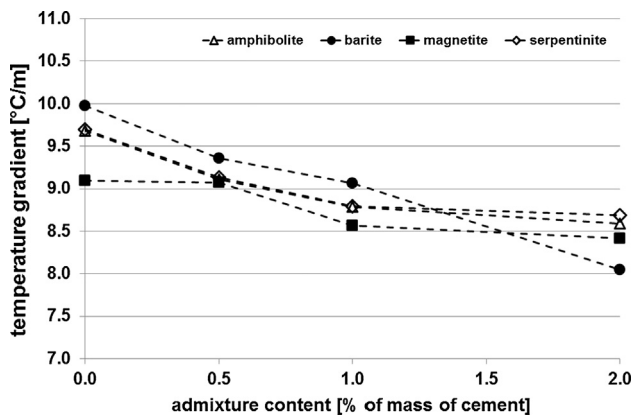

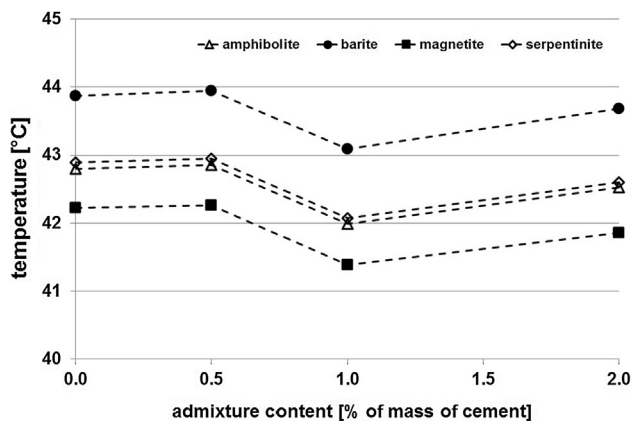**Fig. 11.** Values of the maximum gradient of temperature obtained from the simulations.

Fig. 12. The maximum values of the temperature obtained from the simulations.

3.3. Comsol simulations

The results of simulations carried out using the Comsol program, based on the results obtained from measurements in an isothermal calorimeter, showed a differentiation, depending on the thermal properties of the concrete, in the effect of the admixture used. The results are shown in Figs. 11 and 12, and also in Table 7.

The results obtained from the isometric calorimeter differed slightly from those obtained from experimental measurements performed in the tube. This was reflected in the simulation results. It is visible if we compare the maximum values of the instantaneous temperature rise in the simulated blocks, which are presented in Table 7 for the mixture with serpentinite aggregate. The same values, recorded for the tube measurements, are shown in Table 5.

Comparison of the measurement and simulation results indicates the occurrence of a trend of decreasing the maximum rate of temperature increase along with the increasing amount of the used admixture. In the case of the simulation, which was based on the results of calorimetric measurements, this trend is clearly weakened in the case of the C20 concrete mix, and this may indicate the exhaustion of the potential of the admixture to further reduce the rate of temperature increase. In the experimental results, the trend collapse appears in the graph between the results obtained for the C05 and C10 concrete mixtures. Considering a very large drop in the rate of instantaneous temperature increase in the case of the C05 mixture in relation to the reference mixture, it should be assumed that in the case of the first of them the results differ from the expected ones and should therefore be considered doubtful. For this reason, the results obtained in the isothermal calorimeter were later used for the simulation. Determining the cause of obtaining dubious results requires additional research.

However, in both analysed cases, the trend of delaying the time of reaching the maximum instantaneous temperature increase is equally clear. This delay is greater and increases faster in the case of the results obtained from the simulations than in the case of the experimental results. This is probably due to the specificity of the calorimetric test, which was carried out under isothermal conditions using a cement paste sample of about 120 g. The heat emitted by the hydrating cement in the calorimeter was discharged much faster and more efficiently than in the case of the mixture placed in the tube. This suggests a synergistic effect of lowering the temperature and using the admixture to delay the time of reaching the maximum instantaneous temperature increase.

In all simulated cases, the admixture also caused a decrease in the maximum temperature gradient, which can be seen in Fig. 8. The largest decrease was obtained in the case of the concrete with barite aggregate, where in the case of an admixture content equal to 2.0% the temperature gradient dropped from 10.0°C/m to 8.0°C/m, i.e. by 20%. The smallest decrease was observed in the case of the concrete with magnetite aggregate, where the gradient decreased

Table 7
The maximum instantaneous temperature rise and the time of its occurrence (simulations – mixture with serpentinite aggregate).

Parameter	Measurement point	Mixture designation			
		C0	C05	C10	C20
Max. value of $\Delta T/t$ [°C/h]	1	1.74	1.62	1.43	1.41
	2	1.76	1.63	1.43	1.39
	3	1.64	1.52	1.33	1.30
	4	1.71	1.59	1.40	1.38
The time of max. $\Delta T/t$ [h]	1	12.1	21.7	32.9	54.2
	2	11.9	21.6	32.9	54.4
	3	11.7	21.4	32.7	54.6
	4	12.1	21.7	32.9	54.4

from 9.1°C/m to 8.4°C/m (about 8%). In the cases of the concrete with amphibolite and serpentinite, the gradient values fell in a very similar way and the decrease was moderate.

The obtained results are consistent with the values of the thermal parameters of the concrete in the simulated blocks obtained from the research. The concrete with barite aggregate is characterized by the lowest value of thermal conductivity among the analysed concrete mixtures, as well as the lowest value of specific heat. On one hand, it makes it difficult to exchange heat inside the material between its cooled surface and the interior, and on the other hand, it favours a rapid increase of temperature. The situation is different in the case of the concrete with magnetite aggregate, which is not only characterized by an equally low value of specific heat, but also by the highest value of thermal conductivity among the investigated concrete mixtures. As a result, the heat generated inside the block is quickly transported towards the cooler surface and the resulting temperature gradient is lower.

Confirmation of the above-mentioned relationship is a graph presented in Fig. 12, which shows the maximum temperature values that were achieved in each analysed case during the simulations. Regardless of the content of admixture, the highest temperature was recorded in the case of the concrete with barite aggregate, and the lowest temperature was recorded for that with magnetite aggregate. In the cases of the concrete with serpentinite aggregate and amphibolite aggregate, intermediate results, very similar to each other, were obtained. It should be emphasized, however, that the differences in the maximum values between the individual mixtures are small and do not exceed 2 °C, i.e. about 5%.

Analysis of the maximum temperature graphs shown in Fig. 9 also leads to the conclusion that the influence of the admixture on the obtained maximum temperature value is generally negligible. It did, however, have a slightly more pronounced effect in the case of an admixture in the amount of 1.0%, when the temperature dropped for all mixtures by about 1 °C in relation to blends without admixture. However, this decrease was only about 0.5 °C with the use of admixture in an amount of 2.0%.

4. Conclusions

1. The tested retarding admixture clearly reduces the maximum temperature gradient in the shielding concrete. This was confirmed by both the experimental tests and the computer simulations. The tests also showed that the admixture lowers the rate of temperature increase in concrete.
2. In the experimental tests, performed using concrete with serpentinite aggregate, the gradient was reduced by 18.4% and dropped from 14.7°C/m for the concrete without admixture to 12.0°C/m in the case of the concrete with an admixture dose of 2.0% of cement mass.
3. Computer simulations confirmed that the gradient change in a massive concrete element, resulting from the use of the retarding admixture, depends to a large extent on the thermal properties of the aggregate. They also showed that the greatest decrease occurred in the case of barite aggregate (20.0% from 10.0°C/m to 8.0°C/m), and the smallest decrease was in the case of magnetite aggregate (7.7% from 9.1°C/m to 8.4°C/m).
4. The results of the simulations indicate that the admixture has a slight influence on the maximum value of the temperature obtained in the massive concrete elements regardless of the aggregate used. Differences of the maximum temperature reached in the simulations oscillate at around 2% and are smaller than the differences in the maximum values of temperatures in the concrete with various aggregates, which amount to 4%. In

the latter case, the highest temperature was obtained for the concrete with barite aggregate, and the lowest temperature obtained was for the concrete with magnetite aggregate.
5. Measurements of the temperature of the hardening concrete during experimental tests showed no significant effect of the tested admixture on the obtained maximum temperature rise value.

Conflict of interest

None declared.

Ethical statement

Authors state that the research was conducted according to ethical standards.

Acknowledgements

References

[1] I.S. Bell, P.V. Coveney, Molecular modelling of the mechanism of action of borate retarders on hydrating cements at high temperature, Mol. Simul. 20 (1998) 331–356, https://doi.org/10.1080/08927029808022042.
[2] A.U. Ozturk, B. Baradan, Effects of admixture type and dosage on microstructural and mechanical properties of cement mortars, KSCE J. Civ. Eng. 15 (2011) 1237–1243, https://doi.org/10.1007/s12205-011-0962-x.
[3] E. Tkaczewska, E. Kłosek-Wawrzyn, Effect of phosphate PO4 3- ions on cement hydration, Cement Wapno Beton (2012) 401–408.
[4] W. Nocuń-Wczelik, P. Czapik, Use of calorimetry and other methods in the studies of water reducers and set retarders interaction with hydrating cement paste, Constr. Build. Mater. 38 (2013) 980–986, https://doi.org/10.1016/j.conbuildmat.2012.09.048.
[5] H. Tan, F. Zou, M. Liu, B. Ma, Y. Guo, S. Jian, Effect of the adsorbing behavior of phosphate retarders on hydration of cement paste, J. Mater. Civ. Eng. 29 (2017) 04017088, https://doi.org/10.1061/(ASCE)MT.1943-5533.0001929.
[6] J. Gajda, M. VanGeem, Controlling temperatures in mass concrete, Concr. Int. 24 (2002) 58–62.
[7] M. Briffaut, F. Benboudjema, J.M. Torrenti, G. Nahas, Effects of early-age thermal behaviour on damage risks in massive concrete structures, Eur. J. Environ. Civ. Eng. 16 (2012) 589–605, https://doi.org/10.1080/19648189.2012.668016.
[8] Z. Bofang, Thermal Stresses and Temperature Control of Mass Concrete, Butterworth-Heinemann, 2014.
[9] F. Benboudjema, J.M. Torrenti, Early-age behaviour of concrete nuclear containments, Nucl. Eng. Des. 238 (2008) 2495–2506, https://doi.org/10.1016/j.nucengdes.2008.04.009.
[10] J. Zreiki, F. Bouchelaghem, M. Chaouche, Early-age behaviour of concrete in massive structures, experimentation and modelling, Nucl. Eng. Des. 240 (2010) 2643–2654, https://doi.org/10.1016/j.nucengdes.2010.07.010.
[11] K.A. Riding, J.L. Poole, A.K. Schindler, M.C.G. Juenger, K.J. Folliard, Evaluation of temperature prediction methods for mass concrete members, ACI Mater. J. 103 (2006) 357–365.
[12] G. Knor, Identification, modelling and control of temperature fields in concrete structures, in: Institute of Fundamental Technical Research Polish Academy of Sciences, Warsaw, PhD thesis (in Polish), 2014, p. 215.
[13] W. Zhou, C. Feng, X. Liu, S. Liu, C. Zhang, W. Yuan, Contrastive numerical investigations on thermo-structural behaviors in mass concrete with various cements, Materials (Basel) 9 (2016) 1–19, https://doi.org/10.3390/ma9050378.
[14] K.H. Yang, J.S. Mun, D.G. Kim, M.S. Cho, Comparison of strength-maturity models accounting for hydration heat in massive walls, Int. J. Concr. Struct. Mater. 10 (2016) 47–60, https://doi.org/10.1007/s40069-016-0128-9.
[15] L. Wang, H.Q. Yang, S.H. Zhou, E. Chen, S.W. Tang, Mechanical properties, long-term hydration heat, shinkage behavior and crack resistance of dam concrete designed with low heat Portland (LHP) cement and fly ash, Constr. Build. Mater. 187 (2018) 1073–1091, https://doi.org/10.1016/j.conbuildmat.2018.08.056.

[16] D. Marchon, S. Kawashima, H. Bessaies-Bey, S. Mantellato, S. Ng, Hydration and rheology control of concrete for digital fabrication: Potential admixtures and cement chemistry, Cem. Concr. Res. 112 (2018) 96–110, https://doi.org/10.1016/j.cemconres.2018.05.014.

[17] B. Klemczak, M. Batog, Z. Giergiczny, A. Zmij, Complex effect of concrete composition on the thermo-mechanical behaviour of mass concrete, Materials (Basel) 11 (2018) 1–18, https://doi.org/10.3390/ma11112207.

[18] W. Prince, M. Edwards-Lajnef, P.C. Aïtcin, Interaction between ettringite and a polynaphthalene sulfonate superplasticizer in a cementitious paste, Cem. Concr. Res. 32 (2002) 79–85, https://doi.org/10.1016/S0008-8846(01)00632-9.

[19] V.F. Rahhal, Z. Pavlík, A. Tironi, C.C. Castellano, M.A. Trezza, R. Černý, E.F. Irassar, Effect of cement composition on the early hydration of blended cements with natural zeolite, J. Therm. Anal. Calorim. 128 (2017) 721–733, https://doi.org/10.1007/s10973-016-6007-4.

[20] M. Keppert, L. Scheinherrová, M. Jerman, B. Doušová, L. Kobera, J. Brus, R. Černý, Hydration of ordinary portland cement in presence of lead sorbed on ceramic sorbent, Materials (Basel) 12 (2018) 1–19, https://doi.org/10.3390/ma12010019.

[21] G. Knor, M.A. Glinicki, J. Holnicki-Szulc, Determination of thermal parameters of hardening concrete by means of inverse problem solution, Roads and Bridges - Drogi i Mosty 11 (2012) 281–294, https://doi.org/10.7409/rabdim.012.002.

[22] T. Baran, M.A. Glinicki, D. Jóźwiak-Niedźwiedzka, The properties of special cements for shielding constructions in nuclear power plants, Cement Wapno Beton 21 (2016) 207–215.

[23] A. Długosz, I. Pokorska, M.A. Glinicki, R. Jaskulski, Identification of thermal properties of hardening concrete by means of evolutionary algorithms, Comput. Assist. Methods Eng. Sci. 24 (2017) 101–111.

[24] R. Jaskulski, M.A. Glinicki, W. Kubissa, M. Dąbrowski, Application of a non-stationary method in determination of the thermal properties of radiation shielding concrete with heavy and hydrous aggregate, Int. J. Heat Mass Transf. (2019), https://doi.org/10.1016/j.ijheatmasstransfer.2018.07.050.

[25] B. Kuriakose, B.N. Rao, G.R. Dodagoudar, V. Venkatachalapathy, Modelling of heat of hydration for thick concrete constructions – A note, J. Struct. Eng. 42 (2015) 348–357.

[26] B. Kuriakose, B.N. Rao, G.R. Dodagoudar, Early-age temperature distribution in a massive concrete foundation, Procedia Technol. 25 (2016) 107–114, https://doi.org/10.1016/j.protcy.2016.08.087.

[27] Y.R. Zhang, X.M. Kong, Z.B. Lu, Z.C. Lu, S.S. Hou, Effects of the charge characteristics of polycarboxylate superplasticizers on the adsorption and the retardation in cement pastes, Cem. Concr. Res. 67 (2015) 184–196, https://doi.org/10.1016/j.cemconres.2014.10.004.

[28] Y. He, X. Zhang, R.D. Hooton, Effects of organosilane-modified polycarboxylate superplasticizer on the fluidity and hydration properties of cement paste, Constr. Build. Mater. 132 (2017) 112–123, https://doi.org/10.1016/j.conbuildmat.2016.11.122.

[29] E. Tkaczewska, Effect of the superplasticizer type on the properties of the fly ash blended cement, Constr. Build. Mater. 70 (2014) 388–393, https://doi.org/10.1016/j.conbuildmat.2014.07.096.

[30] N.S. Msinjili, W. Schmidt, B. Mota, S. Leinitz, H.C. Kühne, A. Rogge, The effect of superplasticizers on rheology and early hydration kinetics of rice husk ash-blended cementitious systems, Constr. Build. Mater. 150 (2017) 511–519, https://doi.org/10.1016/j.conbuildmat.2017.05.197.